

Impact of Data Distribution on Fairness Guarantees in Equitable Deep Learning

Yan Luo^{*}, Member, IEEE, Congcong Wen^{*}, Member, IEEE, Min Shi, Member, IEEE, Hao Huang, Yi Fang[†], Member, IEEE, and Mengyu Wang[†], Member, IEEE

Abstract—We present a comprehensive theoretical framework analyzing the relationship between data distributions and fairness guarantees in equitable deep learning. Our work establishes novel theoretical bounds that explicitly account for data distribution heterogeneity across demographic groups, while introducing a formal analysis framework that minimizes expected loss differences across these groups. We derive comprehensive theoretical bounds for fairness errors and convergence rates, and characterize how distributional differences between groups affect the fundamental trade-off between fairness and accuracy. Through extensive experiments on diverse datasets, including FairVision (ophthalmology), CheXpert (chest X-rays), HAM10000 (dermatology), and FairFace (facial recognition), we validate our theoretical findings and demonstrate that differences in feature distributions across demographic groups significantly impact model fairness, with performance disparities particularly pronounced in racial categories. The theoretical bounds we derive corroborate these empirical observations, providing insights into the fundamental limits of achieving fairness in deep learning models when faced with heterogeneous data distributions. This work advances our understanding of fairness in AI-based diagnosis systems and provides a theoretical foundation for developing more equitable algorithms. The code for analysis is publicly available via https://github.com/Harvard-Ophthalmology-AI-Lab/fairness_guarantees.

Index Terms—Fairness Learning, Equitable Deep Learning, Theoretical Fairness Analysis



1 Introduction

Fairness in machine learning has become an increasingly important concern, especially in high-stakes applications such as healthcare, where biased predictions can have severe consequences [1]. Equitable deep learning aims to ensure that predictive models perform equally well across various demographic groups, regardless of factors such as gender, race, and ethnicity [2]. However, achieving fairness guarantees in deep learning models is a challenging task, as it requires careful consideration of the variations in data distribution and the positive sample rate across different groups [3].

Recent work has focused on developing fairness-aware learning algorithms and analyzing their theoretical properties. For example, Zietlow *et al.* [4] formulate the fairness problem as minimizing the absolute difference in the expected per-group error between two groups. Also, the fairness problem in predictive ability has been formalized as minimizing the difference in the expected loss across all demographic groups [5]. This definition provides a mathematical framework for studying fairness in machine learning models and has been used to derive various fairness error bounds and

convergence guarantees [6], [7]. However, while existing strategies have improved model fairness to some extent, there has been limited theoretical analysis of the relationship between data distributions and fairness guarantees [8]. The implications of biases are particularly concerning in high-stakes applications, where unfair assessments can perpetuate systemic inequalities, affect individual opportunities, and erode public trust in automated decision systems [9].

In addition, previous research has investigated the relationship between data distribution, class prevalence, and fairness in machine learning [8], [10]. For example, Hajian and Domingo-Ferrer examine how class imbalance affects the fairness of classification models [10], revealing that performance can vary significantly across different groups when class distribution is uneven. Similarly, Chouldechova explores the impact of data distribution on the fairness of risk assessment models in the criminal justice system [8], demonstrating that the choice of training data distribution can substantially influence the fairness properties of the resulting model. However, these studies primarily focus on specific applications without providing a comprehensive theoretical framework for understanding how differences in class prevalence and feature distributions across demographic groups affect fairness guarantees in general machine learning contexts.

Building upon these insights, this work aims to provide a comprehensive theoretical analysis of the impact of data distribution on the fairness guarantees of equitable deep learning models. By leveraging the fairness problem formulation (Definition 3.1) and the theoretical results on fairness error bounds (Theorem 3.4), convergence rates (Theorem 3.14), and group-specific risk bounds (Theorem 3.17), we derive new analytical bounds that explicitly account

- Yan Luo and Mengyu Wang are with the Harvard Ophthalmology AI Lab at Harvard University, Boston, MA, USA. E-Mails: {ylo16, mengyu_wang}@meei.harvard.edu.
- Congcong Wen, Hao Huang, and Yi Fang are with Embodied AI and Robotics (AIR) Lab at New York University, New York, NY, USA. E-Mails: {wenc, hh1845, yfang}@nyu.edu
- Min Shi is with the School of Computing and Informatics, University of Louisiana at Lafayette, LA USA. E-Mail: min.shi@louisiana.edu.
- * Contributed equally as co-first authors.
- † Contributed equally as co-senior authors.

Manuscript received December XX, 2024; revised July XX, 202X.

for the heterogeneity in data distributions across demographic groups. These bounds provide a deeper understanding of the factors that influence the fairness properties of deep learning models and can guide the development of more robust and equitable algorithms.

The main contributions of this work are as follows:

- We formalize the fairness problem in terms of minimizing the differences in expected loss across various demographic groups, such as race categories, and introduce assumptions on data distributions and loss functions.
- We derive a series of theorems that establish fairness error bounds, algorithmic complexity, generalization bounds, convergence rates, and group-specific risk bounds under various assumptions on the data distributions and loss functions. These results shed light on the key factors influencing the fairness properties of the learned models and provide insights into the design of more robust and equitable algorithms.
- We prove that under certain conditions, the local optima of the fairness problem can outperform those of the supervised learning problem, highlighting the importance of considering fairness criteria in model development.
- We corroborate our theoretical findings with empirical results on diverse datasets, such as FairVision [11], CheXpert [12] HAM10000 [13] and FairFace [14], demonstrating the impact of data distributions on the equitable performance of deep learning models for tasks such as glaucoma screening.

The rest of this paper is organized as follows. In Section 2, we discuss related work on fairness learning and datasets. Section 3 presents our main theoretical results on the impact of data distribution on fairness guarantees. In Section 4, we discuss the empirical validation of the theoretical findings on FairVision and CheXpert. Section 5 concludes the paper and outlines directions for future research. Additionally, in the Appendix, we provide supplementary theoretical proofs and experimental results on the HAM10000 and FairFace datasets.

2 Related Work

2.1 Fairness Learning

In recent years, machine learning has achieved exceptional performance across various fields, yet it often produces biased predictions against different demographic groups. To address this issue, fairness learning has been proposed to eliminate or reduce discrimination and bias against certain protected groups, ensuring fair treatment across different groups. Existing fairness learning approaches can generally be categorized into three strategies: *pre-processing*, which balances the dataset through sampling [15], [16] or generative models [17]; *in-processing*, which incorporates constraints into the loss function [18]; and *post-processing*, which transforms the model output to ensure fairness [19], [20].

However, while these strategies have improved model fairness to some extent, there has been limited theoretical analysis of fairness learning. [9] demonstrates that the trade-off between improving public safety and satisfying current

notions of algorithmic fairness can be achieved through theoretical proof and empirical analysis on Broward County, Florida’s crime data. Additionally, [21] shows that increasing treatment disparity can enhance impact parity through theoretical analysis on simulated and real-world educational data. Recently, [22] proposes a novel fair representation learning method, which achieves non-separability in latent distribution w.r.t. sensitive features by regularizing data distribution and increases separability w.r.t. the target label by maximizing the marginal distance of decision boundaries among different classes. In contrast to the prior works, this work focuses on the implications of the theoretical findings on fairness error bounds, algorithmic complexity, generalization bounds, convergence rates, and group-specific risk bounds.

2.2 Fairness Dataset

Fairness learning has been extensively studied across various fields, with several fairness datasets being proposed in areas such as finance [23], [24], criminology [25], social sciences [26], and education [27], [28]. Among these fields, healthcare stands out as a critically high-stakes domain where biased predictions can lead to significant and far-reaching consequences. To address fairness comprehensively, we leverage both medical and non-medical datasets to capture a wide range of contexts and challenges.

In the medical domain, several datasets exist for fairness learning [12], [13], [29], [30], [31], [32], [33], [34], [35]. However, most suffer from limitations such as small sample sizes (up to several hundred patients), which hinder robust fairness assessment, or restricted demographic attributes like age and gender, which constrain their utility for comprehensive fairness studies. Among the large-scale datasets particularly suited for fairness learning, the FairVision [11] dataset includes 30,000 fundus photos from 30,000 patients, covering three major eye diseases: age-related macular degeneration, diabetic retinopathy, and glaucoma. It offers extensive demographic attributes, including age, gender, race, ethnicity, preferred language, and marital status, making it highly relevant for fairness studies. The CheXpert [12] dataset provides 224,316 chest radiographs of 65,240 patients with labels for 14 common chest radiographic observations, as well as age, gender, and race attributes essential for fairness learning. Similarly, the HAM10000 dataset includes 9,948 dermatoscopic images of pigmented skin lesions with detailed annotations for seven diagnostic categories and metadata for age and gender, making it suitable for fairness studies in skin lesion classification.

Beyond the medical domain, we also utilize datasets like FairFace, which contains 152,917 facial images from 6,100 unique identities annotated with protected attributes such as gender and skin color. FairFace serves as a critical benchmark for evaluating fairness in computer vision models, enabling a broader exploration of fairness issues in non-medical applications. By incorporating both medical and non-medical datasets, we aim to provide a holistic evaluation of fairness across diverse domains, addressing unique challenges in healthcare while extending the analysis to other high-impact areas.

3 Main Results

In this section, we present our main theoretical results on the impact of data distribution on the fairness guarantees. We provide a series of theorems that establish fairness error bounds, algorithmic complexity, generalization bounds, convergence rates, and group-specific risk bounds under various assumptions on the data distributions and loss functions. These results shed light on the key factors influencing the fairness properties of the learned models and provide insights into the design of more robust and equitable algorithms.

A central question in equitable deep learning is how to formalize the notion of fairness in the context of predictive models. Building upon the insights and the fairness problem formulation introduced by [4], we extend the formulation to multiple groups and introduce the fairness problem in predictive ability as minimizing the difference in the expected loss across all demographic groups.

Definition 3.1 (Fairness Problem). *Given an image x , its corresponding label y , a demographic attribute $a \in \{a_1, a_2, \dots, a_k\}$ (e.g., race attributes such as Asian, Black, and White), a function f mapping x to predicted labels \hat{y} , and a loss function ℓ , the fairness problem in predictive ability is defined as minimizing the difference in the expected loss across all demographic groups:*

$$\min_{f(\cdot)} \max_{i,j} \left| \mathbb{E}_{(x,y) \sim \mathcal{D}_{a_i}} [\ell(f(x), y)] - \mathbb{E}_{(x,y) \sim \mathcal{D}_{a_j}} [\ell(f(x), y)] \right| \quad (1)$$

where \mathcal{D}_{a_i} represents the data distribution for demographic group a_i , and $\mathbb{E}_{(x,y) \sim \mathcal{D}_{a_i}} [\cdot]$ denotes the expectation over the data distribution for group a_i .

In real-world applications, we have the optimization objective $\min_{f \in \mathcal{F}} \{L(f(x), y) + \lambda \cdot \max_{i,j} |\mathbb{E}_{(x,y) \sim \mathcal{D}_{a_i}} [\ell(f(x), y)] - \mathbb{E}_{(x,y) \sim \mathcal{D}_{a_j}} [\ell(f(x), y)]|\}$, where $L(f(x), y)$ is a task-specific loss. To clearly understand the fairness problem, we focus on the fairness term (1) in this work.

Definition 3.1 formalizes the fairness problem in predictive ability for a machine learning model. The chain of logic is as follows: Firstly, we have an image x , its corresponding true label y , and a demographic attribute a which can take on values from $\{a_1, a_2, \dots, a_k\}$. For example, the demographic attribute could be race, with categories like Asian, Black, and White. Then, we have a function f that maps the image x to a predicted label \hat{y} , and a loss function ℓ that measures the difference between the predicted label and the true label. Next, the goal is to minimize the maximum absolute difference in the expected loss across all demographic groups. In other words, we want the model to perform equally well (in terms of the loss function) for all demographic groups. The expectation $\mathbb{E}_{(x,y) \sim \mathcal{D}_{a_i}} [\ell(f(x), y)]$ represents the average loss for demographic group a_i , where the data (image-label pairs) are sampled from the distribution \mathcal{D}_{a_i} specific to that group. Finally, by minimizing the maximum absolute difference in the expected loss across all pairs of demographic groups, we ensure that the model's predictive ability is as similar as possible across the groups. This helps mitigate potential biases or unfairness in the model's performance.

Theorem 3.2 (Connection with Conventional Fairness). *Let f be a classifier, ℓ be a loss function bounded by M , and \mathcal{D}_{a_i} be the data distribution for demographic group a_i . Let p_i be the proportion of positive samples in group a_i . Then, for any pair of groups a_i and a_j :*

$$\left| \mathbb{E}_{(x,y) \sim \mathcal{D}_{a_i}} [\ell(f(x), y)] - \mathbb{E}_{(x,y) \sim \mathcal{D}_{a_j}} [\ell(f(x), y)] \right| \leq \max\{p_i, p_j\} \cdot |L^{+,a_i}(f) - L^{+,a_j}(f)| + 2M |p_i - p_j| + \min\{1 - p_i, 1 - p_j\} \cdot |L^{-,a_i}(f) - L^{-,a_j}(f)|$$

where $L^{+,a_k}(f) = \mathbb{E}[\ell(f(x), y) | y = 1, s = a_k]$ is the risk of the positive labeled samples in group a_k , and $L^{-,a_k}(f) = \mathbb{E}[\ell(f(x), y) | y = 0, s = a_k]$ is the risk of the negative labeled samples in group a_k . $L^{+,a_k}(f)$ and $L^{-,a_k}(f)$ are defined in [36].

Proof. First, we decompose the expected loss for each group into positive and negative components:

$$\mathbb{E}_{(x,y) \sim \mathcal{D}_{a_k}} [\ell(f(x), y)] = p_k \cdot L^{+,a_k}(f) + (1 - p_k) \cdot L^{-,a_k}(f)$$

where $k \in \{i, j\}$.

Now, consider the difference in expected losses:

$$\begin{aligned} & \left| \mathbb{E}_{(x,y) \sim \mathcal{D}_{a_i}} [\ell(f(x), y)] - \mathbb{E}_{(x,y) \sim \mathcal{D}_{a_j}} [\ell(f(x), y)] \right| \\ &= |(p_i \cdot L^{+,a_i}(f) + (1 - p_i) \cdot L^{-,a_i}(f)) - (p_j \cdot L^{+,a_j}(f) + (1 - p_j) \cdot L^{-,a_j}(f))| \\ &= |p_i \cdot L^{+,a_i}(f) - p_j \cdot L^{+,a_j}(f) + (1 - p_i) \cdot L^{-,a_i}(f) - (1 - p_j) \cdot L^{-,a_j}(f)| \\ &= |p_i \cdot (L^{+,a_i}(f) - L^{+,a_j}(f)) + (p_i - p_j) \cdot L^{+,a_j}(f) + (1 - p_j) \cdot (L^{-,a_i}(f) - L^{-,a_j}(f)) + (p_j - p_i) \cdot L^{-,a_i}(f)| \\ &= \leq p_i \cdot |L^{+,a_i}(f) - L^{+,a_j}(f)| + |p_i - p_j| \cdot |L^{+,a_j}(f)| + (1 - p_j) \cdot |L^{-,a_i}(f) - L^{-,a_j}(f)| + |p_j - p_i| \cdot |L^{-,a_i}(f)| \end{aligned}$$

Note that $p_i \leq \max\{p_i, p_j\}$ and $(1 - p_j) \leq \min\{1 - p_i, 1 - p_j\}$. Also, since ℓ is bounded by M , we have $|L^{+,a_j}(f)| \leq M$ and $|L^{-,a_i}(f)| \leq M$. Apply these bounds:

$$\begin{aligned} & \max\{p_i, p_j\} \cdot |L^{+,a_i}(f) - L^{+,a_j}(f)| + M |p_i - p_j| \\ &+ \min\{1 - p_i, 1 - p_j\} \cdot |L^{-,a_i}(f) - L^{-,a_j}(f)| + M |p_j - p_i| \\ &\leq \max\{p_i, p_j\} \cdot |L^{+,a_i}(f) - L^{+,a_j}(f)| + 2M |p_i - p_j| \\ &+ \min\{1 - p_i, 1 - p_j\} \cdot |L^{-,a_i}(f) - L^{-,a_j}(f)| \end{aligned}$$

This completes the proof. \square

Remark. Theorem 3.2 establishes a fundamental connection between the fairness problem 3.1 and conventional group-specific performance metrics, showing that differences in expected loss arise from an interplay between the model's group-specific performance characteristics and the underlying class distributions. It suggests that achieving fairness requires careful consideration of both these factors, and that fairness assessments should account for natural demographic variations in class distributions.

The *positive sample rate* (or the proportion of positive samples) plays a significant role in the fairness of machine learning models, particularly in classification tasks. When this rate differs significantly across subgroups, it can introduce or amplify biases, leading to fairness concerns. For example, if a subgroup is underrepresented in the dataset, the model may perform poorly for that group due to insufficient positive

examples for training. Conversely, overrepresentation of a subgroup can dominate the model's learning process, resulting in biased predictions and disparate performance metrics (e.g., accuracy, precision, recall) across groups. Therefore, the positive sample rate is a critical factor in ensuring fairness in machine learning models. Disparities in this rate can lead to biased predictions, unequal outcomes, and reduced trustworthiness of AI systems.

Assumption 3.3 (Bounded Loss and Positive Sample Rate). *Let r_i be the positive sample rate for demographic group a_i , where $\sum_{i=1}^k r_i = 1$. Assume that the loss function ℓ is bounded, i.e., $0 \leq \ell(\hat{y}, y) \leq M$ for some constant $M > 0$.*

Theorem 3.4 (Fairness Error Bound). *Under Assumption 3.3, given the fairness problem as defined in Definition 3.1, let f^* be the optimal function that minimizes the maximum absolute difference in the expected loss across all demographic groups. Let \hat{f} be an estimate of f^* based on a finite sample of size n , and assume that $\|f - f^*\|_\infty \leq \epsilon$ for some $\epsilon > 0$. Then, by Hoeffding's inequality, with probability at least $1 - \delta$, the following inequality holds:*

$$\begin{aligned} & \max_{i,j} |E_{(x,y) \sim D_{a_i}}[\ell(\hat{f}(x), y)] - E_{(x,y) \sim D_{a_j}}[\ell(\hat{f}(x), y)]| \leq \\ & \max_{i,j} |E_{(x,y) \sim D_{a_i}}[\ell(f(x), y)] - E_{(x,y) \sim D_{a_j}}[\ell(f(x), y)]| + \\ & M \sqrt{\frac{\log(2k/\delta)}{2n \min r_i}} + 2L\epsilon \end{aligned}$$

where L is the Lipschitz constant of the loss function ℓ .

Proof. Let $L_i(f) = E_{(x,y) \sim D_{a_i}}[\ell(f(x), y)]$ be the expected loss for demographic group a_i under function f . Define $\Delta(f) = \max_{i,j} |L_i(f) - L_j(f)|$ as the maximum absolute difference in the expected loss across all demographic groups. By the triangle inequality:

$$\begin{aligned} |\Delta(\hat{f}) - \Delta(f^*)| & \leq \max_{i,j} |L_i(\hat{f}) - L_j(\hat{f}) - (L_i(f^*) - L_j(f^*))| \\ & \leq \max_{i,j} (|L_i(\hat{f}) - L_i(f^*)| + |L_j(\hat{f}) - L_j(f^*)|) \end{aligned}$$

For any group i , by the Lipschitz continuity of ℓ :

$$\begin{aligned} |L_i(\hat{f}) - L_i(f^*)| & = |E_{(x,y) \sim D_{a_i}}[\ell(\hat{f}(x), y) - \ell(f^*(x), y)]| \\ & \leq E_{(x,y) \sim D_{a_i}}[|\ell(\hat{f}(x), y) - \ell(f^*(x), y)|] \\ & \leq L E_{(x,y) \sim D_{a_i}}[|\hat{f}(x) - f^*(x)|] \\ & \leq L\epsilon \end{aligned}$$

Therefore:

$$|\Delta(\hat{f}) - \Delta(f^*)| \leq 2L\epsilon$$

By Hoeffding's inequality and the proof from the original Theorem 3.4, with probability at least $1 - \delta$:

$$\begin{aligned} \Delta(\hat{f}) & \leq \Delta(f^*) + |\Delta(\hat{f}) - \Delta(f^*)| \\ & \leq \Delta(f^*) + M \sqrt{\frac{\log(2k/\delta)}{2n \min r_i}} + 2L\epsilon \end{aligned}$$

This completes the proof. \square

Remark. Theorem 3.4 provides an upper bound on the fairness error of the estimated function \hat{f} in terms of the optimal fairness error $\Delta(f^*)$ and a term that depends on the sample size n , the number of demographic groups k , the confidence level δ , and the minimum prevalence $\min_i r_i$.

Specifically, the bound suggests that to achieve a smaller fairness error, one should have a larger sample size n , a smaller number of demographic groups k , a higher confidence level $1 - \delta$, and a more balanced distribution of r_i across the groups. This result highlights the importance of collecting sufficient and diverse data from each demographic group to ensure equitable performance.

Definition 3.5 (ϵ -optimal Solution). *For a minimization problem with objective function $\Delta(f)$ and optimal solution $f^* = \arg \min_{f \in \mathcal{F}} \Delta(f)$, we say that $\hat{f} \in \mathcal{F}$ is an ϵ -optimal solution if:*

$$\Delta(\hat{f}) - \Delta(f^*) \leq \epsilon \quad (2)$$

where $\epsilon > 0$ is the optimality gap. In the context of the fairness problem (Definition 3.1), this means:

$$\begin{aligned} & \max_{i,j} |E_{(x,y) \sim D_{a_i}}[\ell(\hat{f}(x), y)] - E_{(x,y) \sim D_{a_j}}[\ell(\hat{f}(x), y)]| \leq \\ & \min_{f \in \mathcal{F}} \max_{i,j} |E_{(x,y) \sim D_{a_i}}[\ell(f(x), y)] - E_{(x,y) \sim D_{a_j}}[\ell(f(x), y)]| + \epsilon \end{aligned}$$

ϵ -optimality is particularly useful in practice when finding the exact optimal solution f^* may be computationally intractable.

Assumption 3.6 (Lipschitz Continuity). *Assume that the loss function ℓ is Lipschitz continuous with respect to its first argument, i.e., there exists a constant $L > 0$ such that $|\ell(\hat{y}_1, y) - \ell(\hat{y}_2, y)| \leq L|\hat{y}_1 - \hat{y}_2|$ for all \hat{y}_1, \hat{y}_2, y .*

Theorem 3.7 (Algorithm Complexity of Fairness Problem). *Under Assumptions 3.3 and 3.6, given the fairness problem as defined in Definition 3.1 with k demographic groups and a function class \mathcal{F} with finite Vapnik-Chervonenkis (VC) dimension d , there exists an algorithm that finds an ϵ -optimal solution \hat{f} to the fairness problem with probability at least $1 - \delta$, using $O(\frac{k^2}{\epsilon^2}(d \log(k/\epsilon) + \log(k/\delta)))$ samples and $O(k^2|\mathcal{F}|)$ time complexity.*

Proof. Let $f^* = \arg \min_{f \in \mathcal{F}} \Delta(f)$ be the optimal solution to the fairness problem, where $\Delta(f) = \max_{i,j} |L_i(f) - L_j(f)|$ is the maximum absolute difference in the expected loss across all demographic groups.

Lemma 3.8 (Uniform Convergence Bound for Fairness Problem). *Let \mathcal{F} be a function class with finite VC dimension d . For any $\epsilon, \delta > 0$, if the sample size n satisfies $n \geq \frac{8M^2k^2}{\epsilon^2}(d \log(16Mk/\epsilon) + \log(4k^2/\delta))$, then with probability at least $1 - \delta$, the following holds for all $f \in \mathcal{F}$ and all pairs of demographic groups (i, j) simultaneously:*

$$|L_i(f) - L_j(f) - (\hat{L}_i(f) - \hat{L}_j(f))| \leq \epsilon/2$$

where $\hat{L}_i(f) = \frac{1}{n_i} \sum_{j=1}^{n_i} \ell(f(x_j^{(i)}), y_j^{(i)})$ is the empirical loss for group a_i , and $n_i = nr_i$ is the sample size for group a_i .

The lemma follows from the standard uniform convergence bound for finite VC dimension function classes, applied to the pairwise differences of the loss functions for each pair of demographic groups. Now, consider the following algorithm:

- 1) Draw a sample of size $n \geq \frac{8M^2k^2}{\epsilon^2}(d \log(16Mk/\epsilon) + \log(4k^2/\delta))$.
- 2) For each $f \in \mathcal{F}$, calculate the empirical fairness error $\hat{\Delta}(f) = \max_{i,j} |\hat{L}_i(f) - \hat{L}_j(f)|$.
- 3) Return $\hat{f} = \arg \min_{f \in \mathcal{F}} \hat{\Delta}(f)$.

By the uniform convergence lemma, with probability at least $1 - \delta$, we have:

$$\begin{aligned} \Delta(\hat{f}) &\leq \hat{\Delta}(\hat{f}) + \epsilon/2 \\ &\leq \hat{\Delta}(f^*) + \epsilon/2 \\ &\leq \Delta(f^*) + \epsilon \end{aligned}$$

Therefore, the algorithm returns an ϵ -optimal solution with probability at least $1 - \delta$. The sample complexity is $O(\frac{k^2}{\epsilon^2}(d \log(k/\epsilon) + \log(k/\delta)))$, and the time complexity is $O(k^2|\mathcal{F}|)$ since we need to calculate the empirical fairness error for each function in \mathcal{F} and each pair of demographic groups. \square

Remark. Theorem 3.6 sheds light on the sample and time complexity of finding an ϵ -optimal fair solution. The sample complexity grows quadratically with the number of demographic groups k and inversely with the square of the desired accuracy ϵ , as we need to ensure uniform convergence for all pairs of demographic groups. Similarly, the time complexity increases by a factor of k^2 due to the pairwise comparisons of the empirical loss functions. These results highlight the challenges in achieving fairness in large-scale applications with multiple demographic groups and complex models.

Lemma 3.9 (Symmetrization). *For any function $f \in \mathcal{F}$,*

$$\mathbb{P}[R(f) - R_{\text{emp}}(f) > \epsilon] \leq 2\mathbb{P}\left[\sup_{f \in \mathcal{F}} |R_{\text{emp}}(f) - R'_{\text{emp}}(f)| > \frac{\epsilon}{2}\right]$$

where $R(f)$ is the true fairness risk, $R_{\text{emp}}(f)$ is the empirical fairness risk on the original sample, and $R'_{\text{emp}}(f)$ is the empirical fairness risk on a ghost sample of size m drawn independently from the same distribution as the original sample.

Proof. Let $S = (x_1, y_1), \dots, (x_m, y_m)$ be the original sample of size m and $S' = (x'_1, y'_1), \dots, (x'_m, y'_m)$ be the ghost sample of size m , both drawn independently from the same distribution. Define the event A as:

$$A = \exists f \in \mathcal{F} : R(f) - R_{\text{emp}}(f) > \epsilon$$

We want to bound the probability of event A . Consider the following event B :

$$B = \left\{ \sup_{f \in \mathcal{F}} |R_{\text{emp}}(f) - R'_{\text{emp}}(f)| > \frac{\epsilon}{2} \right\}$$

We will show that $A \subseteq B \cup B'$, where B' is the same event as B but with the roles of S and S' swapped. Suppose event A occurs, i.e., there exists a function $f \in \mathcal{F}$ such that $R(f) - R_{\text{emp}}(f) > \epsilon$. Then, we have:

$$\begin{aligned} R(f) - R_{\text{emp}}(f) &> \epsilon \\ R(f) - R'_{\text{emp}}(f) + R'_{\text{emp}}(f) - R_{\text{emp}}(f) &> \epsilon \\ [R(f) - R'_{\text{emp}}(f)] + [R'_{\text{emp}}(f) - R_{\text{emp}}(f)] &> \epsilon \end{aligned}$$

If $R(f) - R'_{\text{emp}}(f) \leq \epsilon/2$, then we must have $R'_{\text{emp}}(f) - R_{\text{emp}}(f) > \epsilon/2$, which implies event B occurs. On the other hand, if $R(f) - R'_{\text{emp}}(f) > \epsilon/2$, then by swapping the roles of S and S' , we have $R'_{\text{emp}}(f) - R_{\text{emp}}(f) > \epsilon/2$, which implies

event B' occurs. Therefore, $A \subseteq B \cup B'$, and by the union bound, we have:

$$\mathbb{P}[A] \leq \mathbb{P}[B] + \mathbb{P}[B']$$

Since S and S' are drawn independently from the same distribution, we have $\mathbb{P}[B] = \mathbb{P}[B']$. Thus,

$$\mathbb{P}[A] \leq 2\mathbb{P}[B]$$

which is equivalent to:

$$\mathbb{P}[R(f) - R_{\text{emp}}(f) > \epsilon] \leq 2\mathbb{P}\left[\sup_{f \in \mathcal{F}} |R_{\text{emp}}(f) - R'_{\text{emp}}(f)| > \frac{\epsilon}{2}\right]$$

This completes the proof. \square

Theorem 3.10 (Fairness Generalization Bound). *Under Assumptions 3.3, given the fairness problem as defined in Definition 3.1 with k demographic groups and a function space \mathcal{F} with VC dimension $d_{\text{VC}}(\mathcal{F})$, for any $\delta > 0$, with probability at least $1 - \delta$, for all $f \in \mathcal{F}$:*

$$\begin{aligned} \max_{i,j} |R_i(f) - R_j(f)| &\leq \max_{i,j} |R_{\text{emp},i}(f) - R_{\text{emp},j}(f)| + \\ &M \sqrt{\frac{8(d_{\text{VC}}(\mathcal{F}) \ln(2em/d_{\text{VC}}(\mathcal{F})) + \ln(4k^2/\delta))}{m}} \end{aligned}$$

where $R_i(f) = \mathbb{E}_{(x,y) \sim \mathcal{D}_{a_i}}[\ell(f(x), y)]$ is the expected fair risk for group a_i , $R_{\text{emp},i}(f) = \frac{1}{m_i} \sum_{j=1}^{m_i} \ell(f(x_j^{(i)}), y_j^{(i)})$ is the empirical risk for group a_i , m_i is the sample size for group a_i , and $m = \sum_{i=1}^k m_i$ is the total sample size.

Proof. Let $R(f) = \max_{i,j} |R_i(f) - R_j(f)|$ be the fairness risk and $R_{\text{emp}}(f) = \max_{i,j} |R_{\text{emp},i}(f) - R_{\text{emp},j}(f)|$ be the empirical fairness risk. Based on Lemma 3.9, by the VC dimension bound in the attached file, we have:

$$\mathbb{P}\left[\sup_{f \in \mathcal{F}} |R_{\text{emp}}(f) - R'_{\text{emp}}(f)| > \frac{\epsilon}{2}\right] \leq 4\Phi(2m) \exp\left(-\frac{m\epsilon^2}{8M^2}\right)$$

where $\Phi(m) = \sum_{i=0}^{d_{\text{VC}}(\mathcal{F})} \binom{m}{i}$ is the growth function of \mathcal{F} . Using the bound $\Phi(m) \leq \left(\frac{em}{d_{\text{VC}}(\mathcal{F})}\right)^{d_{\text{VC}}(\mathcal{F})}$ and setting the right-hand side to $\delta/(2k^2)$, we get:

$$\mathbb{P}\left[\sup_{f \in \mathcal{F}} |R_{\text{emp}}(f) - R'_{\text{emp}}(f)| > \frac{\epsilon}{2}\right] \leq \frac{\delta}{2k^2}$$

Applying the union bound over all pairs of demographic groups, we have:

$$\mathbb{P}[\exists i, j : R_i(f) - R_j(f) > \epsilon] \leq \delta$$

provided that:

$$\epsilon = M \sqrt{\frac{8(d_{\text{VC}}(\mathcal{F}) \ln(2em/d_{\text{VC}}(\mathcal{F})) + \ln(4k^2/\delta))}{m}}$$

Therefore, with probability at least $1 - \delta$, for all $f \in \mathcal{F}$:

$$\begin{aligned} \max_{i,j} |R_i(f) - R_j(f)| &\leq \max_{i,j} |R_{\text{emp},i}(f) - R_{\text{emp},j}(f)| + \\ &M \sqrt{\frac{8(d_{\text{VC}}(\mathcal{F}) \ln(2em/d_{\text{VC}}(\mathcal{F})) + \ln(4k^2/\delta))}{m}} \end{aligned}$$

This completes the proof. \square

Corollary 3.11 (Relationship between Upper Bound and Fairness Risk). *Let B_1 and B_2 be two upper bounds derived from Theorem 3.9 such that $B_1 < B_2$. Then,*

for any function $f \in \mathcal{F}$, with probability at least $1 - \delta$: $\max_{i,j} |R_i(f) - R_j(f)| \leq B_1 < B_2$, where B_1 and B_2 are of the form: $B_l = \max_{i,j} |R_{emp,i}(f) - R_{emp,j}(f)| + M \sqrt{\frac{8(d_{VC}(\mathcal{F}) \ln(2em/d_{VC}(\mathcal{F})) + \ln(4k^2/\delta))}{m_l}}$ for $l \in \{1, 2\}$ and $m_1 > m_2$ or $d_{VC,1}(\mathcal{F}) < d_{VC,2}(\mathcal{F})$ or $k_1 < k_2$ or $M_1 < M_2$.

Proof. Let's prove this by analyzing the components of the upper bound from Theorem 3.10. First, note that the bound consists of two terms: empirical fairness risk: $\max_{i,j} |R_{emp,i}(f) - R_{emp,j}(f)|$, and complexity term: $M \sqrt{\frac{8(d_{VC}(\mathcal{F}) \ln(2em/d_{VC}(\mathcal{F})) + \ln(4k^2/\delta))}{m}}$. The complexity term is monotonically: decreasing with respect to sample size m , increasing with respect to VC dimension $d_{VC}(\mathcal{F})$, increasing with respect to number of groups k , or increasing with respect to loss bound M .

Therefore, if B_1 and B_2 are derived under conditions where one or more of: 1) $m_1 > m_2$, 2) $d_{VC,1}(\mathcal{F}) < d_{VC,2}(\mathcal{F})$, 3) $k_1 < k_2$, or 4) $M_1 < M_2$. Then $B_1 < B_2$.

By Theorem 3.10, we know that with probability at least $1 - \delta$: $\max_{i,j} |R_i(f) - R_j(f)| \leq B_1$. By transitivity: $\max_{i,j} |R_i(f) - R_j(f)| \leq B_1 < B_2$

This completes the proof. \square

Remark. Theorem 3.10 (Fairness Generalization Bound) is a key result that provides an upper bound on the fairness risk of a learned model in terms of its empirical fairness risk, the VC dimension of the function space, the number of demographic groups, and the sample size. This bound is crucial for understanding the generalization performance of fair learning algorithms and the factors that influence their ability to produce equitable models. The theorem suggests that to achieve a smaller fairness risk (see Corollary 3.11), one should have a larger sample size, a smaller VC dimension, and a smaller number of demographic groups. These insights are in line with the well-known bias-complexity trade-off in statistical learning theory [37], where models with lower complexity (i.e., smaller VC dimension) tend to have better generalization performance.

Assumption 3.12 (Bounded Loss and Lipschitz Continuity). Assume that the loss function ℓ is bounded, i.e., $0 \leq \ell(\hat{y}, y) \leq M$ for some constant $M > 0$. Furthermore, assume that the loss function ℓ is Lipschitz continuous with respect to its first argument, i.e., there exists a constant $L > 0$ such that $|\ell(\hat{y}_1, y) - \ell(\hat{y}_2, y)| \leq L|\hat{y}_1 - \hat{y}_2|$ for all \hat{y}_1, \hat{y}_2, y .

Lemma 3.13 (Uniform Convergence of Fairness Risk). Under Assumption 3.6, for any $\delta > 0$, with probability at least $1 - \delta$ over the random choice of S :

$$\sup_{f \in \mathcal{F}} |R(f) - R_{emp}(f, S)| \leq \frac{2LM}{\sqrt{m}} \left(\sqrt{2d_{VC}(\mathcal{F}) \ln \frac{em}{d_{VC}(\mathcal{F})}} + \sqrt{2 \ln \frac{4}{\delta}} \right)$$

Proof. Let $\mathcal{G} = (x, y) \mapsto \ell(f(x), y) : f \in \mathcal{F}$ be the function class induced by the loss function ℓ and the function class \mathcal{F} . By Assumption 3.6, the loss function ℓ is bounded by M and Lipschitz continuous with constant L . For any function $g \in \mathcal{G}$, we have:

$$|g(x, y)| = |\ell(f(x), y)| \leq M$$

and for any $(x_1, y_1), (x_2, y_2)$,

$$\begin{aligned} |g(x_1, y_1) - g(x_2, y_2)| &= |\ell(f(x_1), y_1) - \ell(f(x_2), y_2)| \\ &\leq L|f(x_1) - f(x_2)| \\ &\leq LD|x_1 - x_2| \end{aligned}$$

where D is the Lipschitz constant of functions in \mathcal{F} . Therefore, functions in \mathcal{G} are bounded by M and Lipschitz continuous with constant LD . By McDiarmid's inequality, for any $f \in \mathcal{F}$, with probability at least $1 - \delta/2$,

$$|R(f) - R_{emp}(f, S)| \leq M \sqrt{\frac{2 \ln(2/\delta)}{m}}$$

Let $N(\epsilon, \mathcal{F}, |\cdot|_\infty)$ be the ϵ -covering number of \mathcal{F} with respect to the L_∞ norm. By the Lipschitz continuity of the loss function, we have:

$$N(\epsilon, \mathcal{G}, |\cdot|_\infty) \leq N(\epsilon/L, \mathcal{F}, |\cdot|_\infty)$$

By the VC dimension bound on the covering number [38], we have:

$$N(\epsilon/L, \mathcal{F}, |\cdot|_\infty) \leq \left(\frac{2eL}{\epsilon} \right)^{d_{VC}(\mathcal{F})}$$

By the union bound and the covering number bound, with probability at least $1 - \delta/2$, for all $f \in \mathcal{F}$,

$$|R(f) - R_{emp}(f, S)| \leq M \sqrt{\frac{2(d_{VC}(\mathcal{F}) \ln(2eL/\epsilon) + \ln(2/\delta))}{m}}$$

Setting $\epsilon = LM \sqrt{\frac{2d_{VC}(\mathcal{F}) \ln(em/d_{VC}(\mathcal{F}))}{m}}$, we get:

$$\begin{aligned} \sup_{f \in \mathcal{F}} |R(f) - R_{emp}(f, S)| &\leq \\ \frac{2LM}{\sqrt{m}} &\left(\sqrt{2d_{VC}(\mathcal{F}) \ln \frac{em}{d_{VC}(\mathcal{F})}} + \sqrt{2 \ln \frac{4}{\delta}} \right) \end{aligned}$$

with probability at least $1 - \delta$ over the random choice of S . This completes the proof. \square

Theorem 3.14 (Convergence of Fairness Risk Minimizer). Let \mathcal{F} be a function space with VC dimension $d_{VC}(\mathcal{F})$ and let $f^* = \arg \min_{f \in \mathcal{F}} R(f)$ be the fairness risk minimizer. Let $\hat{f}_S = \arg \min_{f \in \mathcal{F}} R_{emp}(f, S)$ be the empirical fairness risk minimizer based on a training set S of size m . Then, under Assumptions 3.3 and 3.6, for any $\delta > 0$, with probability at least $1 - \delta$ over the random choice of S :

$$R(\hat{f}_S) - R(f^*) \leq \frac{2LM}{\sqrt{m}} \left(\sqrt{2d_{VC}(\mathcal{F}) \ln \frac{em}{d_{VC}(\mathcal{F})}} + \sqrt{2 \ln \frac{4}{\delta}} \right)$$

Proof. The proof relies on Lemma 3.13. Let $\epsilon = \frac{2LM}{\sqrt{m}} \left(\sqrt{2d_{VC}(\mathcal{F}) \ln \frac{em}{d_{VC}(\mathcal{F})}} + \sqrt{2 \ln \frac{4}{\delta}} \right)$. By the lemma, with probability at least $1 - \delta$ over the random choice of S :

$$R(\hat{f}_S) \leq R_{emp}(\hat{f}_S, S) + \epsilon \leq R_{emp}(f^*, S) + \epsilon \leq R(f^*) + 2\epsilon$$

Therefore, with probability at least $1 - \delta$ over the random choice of S :

$$R(\hat{f}_S) - R(f^*) \leq \frac{2LM}{\sqrt{m}} \left(\sqrt{2d_{VC}(\mathcal{F}) \ln \frac{em}{d_{VC}(\mathcal{F})}} + \sqrt{2 \ln \frac{4}{\delta}} \right)$$

This completes the proof. \square

Remark. Theorem 3.14 (Convergence of Fairness Risk Minimizer) is a fundamental result that characterizes the convergence rate of the empirical fairness risk minimizer to the true fairness risk minimizer. The theorem shows that the excess fairness risk, defined as the difference between the fairness risk of the empirical minimizer and the true minimizer, converges to zero at a rate of $O(1/\sqrt{m})$, where m is the sample size. The convergence rate has important implications for the sample complexity of fair learning algorithms. It suggests that to achieve a desired level of accuracy, the sample size should grow quadratically with the inverse of the desired accuracy. This sample complexity is higher than that of the standard empirical risk minimization [39], which has a sample complexity of $O(1/\epsilon^2)$ for an accuracy level of ϵ [40]. Moreover, as the size of the training set increases, the empirical fairness risk minimizer approaches the true fairness risk minimizer, ensuring the convergence of the learning algorithm to a fair solution.

Assumption 3.15 (Normal Distribution for Group a_i). Assume that the data distribution for demographic group a_i follows a normal distribution with mean μ_i and covariance matrix Σ_i , i.e., $(x, y) \sim \mathcal{N}(\mu_i, \Sigma_i)$ for $(x, y) \in \mathcal{D}_{a_i}$.

Lemma 3.16 (Risk Bound for Normal Distributions). Let p_i and p be the density functions of two normal distributions with means μ_i and μ , and covariance matrices Σ_i and Σ , respectively. Then, for any function f :

$$\left| \mathbb{E}_{(x,y) \sim p_i}[f(x, y)] - \mathbb{E}_{(x,y) \sim p}[f(x, y)] \right| \leq L_f |\mu_i - \mu|_2 + L_f \sqrt{|\Sigma_i - \Sigma|_F}$$

where L_f is the Lipschitz constant of f with respect to the Euclidean norm.

Proof. Let $\mathcal{P}(\mathbb{R}^d \times \mathbb{R})$ be the set of all probability measures on $\mathbb{R}^d \times \mathbb{R}$, and let $\Pi(p_i, p)$ be the set of all joint probability measures on $(\mathbb{R}^d \times \mathbb{R}) \times (\mathbb{R}^d \times \mathbb{R})$ with marginals p_i and p . The Kantorovich-Rubinstein duality states that for any Lipschitz function f with Lipschitz constant L_f , we have:

$$\left| \mathbb{E}_{(x,y) \sim p_i}[f(x, y)] - \mathbb{E}_{(x,y) \sim p}[f(x, y)] \right| \leq L_f \cdot W_1(p_i, p) \quad (3)$$

where $W_1(p_i, p)$ is the 1-Wasserstein distance between p_i and p , defined as:

$$W_1(p_i, p) = \inf_{\gamma \in \Pi(p_i, p)} \mathbb{E}_{((x,y),(x',y')) \sim \gamma} [|x - x'|_2] \quad (4)$$

Now, let's focus on bounding the 1-Wasserstein distance between two normal distributions $p_i = \mathcal{N}(\mu_i, \Sigma_i)$ and $p = \mathcal{N}(\mu, \Sigma)$. By the triangular inequality, we have:

$$W_1(p_i, p) \leq \inf_{\gamma \in \Pi(p_i, p)} \mathbb{E}_{((x,y),(x',y')) \sim \gamma} [|x - x'|_2] + \quad (5)$$

$$\inf_{\gamma \in \Pi(p_i, p)} \mathbb{E}_{((x,y),(x',y')) \sim \gamma} [|y - y'|_2] \quad (6)$$

$$\leq W_1(\mathcal{N}(\mu_i, \Sigma_i), \mathcal{N}(\mu, \Sigma_i)) + W_1(\mathcal{N}(\mu, \Sigma_i), \mathcal{N}(\mu, \Sigma)) \quad (7)$$

The first term in Eq. (7) can be bounded by the mean difference:

$$W_1(\mathcal{N}(\mu_i, \Sigma_i), \mathcal{N}(\mu, \Sigma_i)) \leq |\mu_i - \mu|_2 \quad (8)$$

The second term in Eq. (7) can be bounded by the covariance difference [41]:

$$W_1(\mathcal{N}(\mu, \Sigma_i), \mathcal{N}(\mu, \Sigma)) \leq \sqrt{|\Sigma_i - \Sigma|_F} \quad (9)$$

Combining Eq. (3), Eq. (7), Eq. (8), and Eq. (9), we obtain:

$$\left| \mathbb{E}_{(x,y) \sim p_i}[f(x, y)] - \mathbb{E}_{(x,y) \sim p}[f(x, y)] \right| \leq L_f |\mu_i - \mu|_2 + L_f \sqrt{|\Sigma_i - \Sigma|_F}$$

which completes the proof. \square

Theorem 3.17 (Group-Specific Risk Bound Theorem for Normal Distributions). Let \mathcal{F} be a function space with VC dimension $d_{VC}(\mathcal{F})$ and let $f_i^* = \arg \min_{f \in \mathcal{F}} R_i(f)$ be the risk minimizer for demographic group a_i . Let $\hat{f}_S = \arg \min_{f \in \mathcal{F}} R_{emp}(f, S)$ be the empirical risk minimizer based on a training set S of size m drawn from the overall data distribution. Then, under Assumptions 3.6 and 3.15, for any $\delta > 0$, with probability at least $1 - \delta$ over the random choice of S :

$$R_i(\hat{f}_S) - R_i(f_i^*) \leq \frac{2LM}{\sqrt{m}} \left(\sqrt{2d_{VC}(\mathcal{F}) \ln \frac{em}{d_{VC}(\mathcal{F})}} + \sqrt{2 \ln \frac{4}{\delta}} \right) + L |\mu_i - \mu|_2 + L \sqrt{|\Sigma_i - \Sigma|_F}$$

where $R_i(f) = \mathbb{E}_{(x,y) \sim \mathcal{D}_{a_i}} [\ell(f(x), y)]$ is the expected risk for group a_i , $R_{emp}(f, S) = \frac{1}{m} \sum_{j=1}^m \ell(f(x_j), y_j)$ is the empirical risk based on the training set S , μ and Σ are the mean and covariance matrix of the overall data distribution, and $|\cdot|_F$ denotes the Frobenius norm.

Remark. Theorem 3.17 establishes that for a specific demographic group a_i with a normal data distribution, the excess risk of the empirical risk minimizer trained on the overall data distribution, $R_i(\hat{f}_S) - R_i(f_i^*)$, can be bounded by three terms: The first term is the same as in Theorem 3.14 and depends on the VC dimension of the function space, the Lipschitz constant of the loss function, the boundedness of the loss function, and the size of the training set S . The second term is proportional to the Euclidean distance between the means of the group-specific distribution and the overall distribution, $|\mu_i - \mu|_2$. The third term is proportional to the square root of the Frobenius norm of the difference between the covariance matrices of the group-specific distribution and the overall distribution, $\sqrt{|\Sigma_i - \Sigma|_F}$. The result implies that the accuracy of the empirical risk minimizer on group a_i depends not only on the size of the training set and the complexity of the function space but also on how close the group-specific distribution is to the overall distribution in terms of their means and covariance matrices. If the means and covariances are similar, the excess risk will be smaller, indicating better accuracy on group a_i . Conversely, if the means and covariances differ significantly, the excess risk will be larger, indicating potential accuracy disparities for group a_i .

The first term depends on the VC dimension of the hypothesis space, the Lipschitz constant of the loss function, the boundedness of the loss function, and the size of the training set S . The second term is proportional to the Euclidean distance between the means of the group-specific distribution and the overall distribution, $|\mu_i - \mu|_2$. The third term is proportional to the square root of the Frobenius norm of the difference between the covariance matrices of the group-specific distribution and the overall distribution, $\sqrt{|\Sigma_i - \Sigma|_F}$.

The result implies that the accuracy of the empirical risk minimizer on group a_i depends not only on the size of the

training set and the complexity of the hypothesis space but also on how close the group-specific distribution is to the overall distribution in terms of their means and covariance matrices. If the means and covariances are similar, the excess risk will be smaller, indicating better accuracy on group a_i . Conversely, if the means and covariances differ significantly, the excess risk will be larger, indicating potential accuracy disparities for group a_i .

Corollary 3.18 (Fairness-Accuracy Trade-off). *Let \mathcal{F} be a function space with VC dimension $d_{VC}(\mathcal{F})$, and let $f^* = \arg \min_{f \in \mathcal{F}} R(f)$ and $f_i^* = \arg \min_{f \in \mathcal{F}} R_i(f)$ be the fairness and accuracy risk minimizers, respectively. Let $\hat{f}_S = \arg \min_{f \in \mathcal{F}} R_{emp}(f, S)$ be the empirical fairness risk minimizer based on a training set S of size m drawn from the overall data distribution. Then, under Assumptions 3.3, 3.6, and 3.15, for any $\delta > 0$, with probability at least $1 - \delta$ over the random choice of S :*

$$R_i(f^*) - R_i(f_i^*) \leq \frac{4LM}{\sqrt{m}} \sqrt{2d_{VC}(\mathcal{F}) \ln \frac{em}{d_{VC}(\mathcal{F})} + 2 \ln \frac{4}{\delta}} + L|\mu_i - \mu|_2 + L\sqrt{|\Sigma_i - \Sigma|_F}$$

Proof. By the triangle inequality and Theorems 3.14 and 3.17, we have:

$$\begin{aligned} R_i(f^*) - R_i(f_i^*) &\leq R_i(f^*) - R_i(\hat{f}_S) + R_i(\hat{f}_S) - R_i(f_i^*) \\ &\leq \frac{2LM}{\sqrt{m}} \sqrt{2d_{VC}(\mathcal{F}) \ln \frac{em}{d_{VC}(\mathcal{F})} + 2 \ln \frac{4}{\delta}} \\ &\quad + \frac{2LM}{\sqrt{m}} \sqrt{2d_{VC}(\mathcal{F}) \ln \frac{em}{d_{VC}(\mathcal{F})} + 2 \ln \frac{4}{\delta}} + \\ &\quad L|\mu_i - \mu|_2 + L\sqrt{|\Sigma_i - \Sigma|_F} \\ &= \frac{4LM}{\sqrt{m}} \sqrt{2d_{VC}(\mathcal{F}) \ln \frac{em}{d_{VC}(\mathcal{F})} + 2 \ln \frac{4}{\delta}} + \\ &\quad L|\mu_i - \mu|_2 + L\sqrt{|\Sigma_i - \Sigma|_F} \end{aligned}$$

This completes the proof. \square

Remark. Corollary 3.18 quantifies the trade-off between fairness and accuracy in equitable deep learning models. The left-hand side of the inequality, $R_i(f^*) - R_i(f_i^*)$, represents the difference in accuracy between the fairness risk minimizer f^* and the accuracy risk minimizer f_i^* for a specific demographic group a_i . The right-hand side provides an upper bound on this difference, which depends on the VC dimension of the function space, the Lipschitz constant of the loss function, the sample size, and the dissimilarity between the group-specific distribution and the overall distribution. This result has important implications for the design and evaluation of fair learning algorithms. It suggests that achieving perfect fairness (i.e., $R_i(f^*) = R_i(f_i^*)$ for all groups) may come at the cost of reduced accuracy, especially when the data distributions differ significantly across demographic groups. Practitioners should carefully consider this trade-off when developing equitable models and assess the impact of fairness constraints on the model's performance for each group [19]. Also, the corollary highlights the importance of collecting representative data from each demographic group to mitigate the accuracy disparities induced by distributional differences. By reducing the dissimilarity between the group-specific distributions and the overall distribution, one can tighten

the fairness-accuracy trade-off and achieve more equitable performance across all groups [2].

Theorem 3.19 (Expected Loss Bound for Demographic Group with Normal Distribution). *Let $\mathcal{D}_{a_i} \sim \mathcal{N}(\mu_i, \Sigma_i)$ be the data distribution for demographic group a_i , and let $\mathcal{D} \sim \mathcal{N}(\mu, \Sigma)$ be the overall data distribution. Let $f(\cdot)$ be a function that maps input x to predicted labels \hat{y} , and let ℓ be a loss function bounded by B , i.e., $|\ell(f(x), y)| \leq B$ for all x, y . Suppose we have a training set $(x_j, y_j)_{j=1}^n$ of size n drawn independently from \mathcal{D} . Then, with probability at least $1 - \delta$, the expected loss of $f(\cdot)$ on \mathcal{D}_{a_i} is bounded as follows:*

$$\mathbb{E}_{(x,y) \sim \mathcal{D}_{a_i}}[\ell(f(x), y)] \leq \mathbb{E}_{(x,y) \sim \mathcal{D}}[\ell(f(x), y)] + B|\mu_i - \mu|_2 + B\sqrt{|\Sigma_i - \Sigma|_F}$$

Proof. We start by applying the reference theorem to the overall data distribution \mathcal{D} :

$$\mathbb{E}_{(x,y) \sim \mathcal{D}}[\ell(f(x), y)] \leq \frac{1}{n} \sum_{j=1}^n \ell(f(x_j), y_j) + B\sqrt{\frac{2|\Sigma| \log(2/\delta)}{n}}$$

Now, we use Lemma 3.16 to relate the expected loss on \mathcal{D}_{a_i} to the expected loss on \mathcal{D} : Applying the lemma with $f(x, y) = \ell(f(x), y)$, which has Lipschitz constant B since ℓ is bounded by B , we have:

$$|\mathbb{E}_{(x,y) \sim \mathcal{D}_{a_i}}[\ell(f(x), y)] - \mathbb{E}_{(x,y) \sim \mathcal{D}}[\ell(f(x), y)]| \leq B|\mu_i - \mu|_2 + B\sqrt{|\Sigma_i - \Sigma|_F}$$

Rearranging the terms, we get:

$$\mathbb{E}_{(x,y) \sim \mathcal{D}_{a_i}}[\ell(f(x), y)] \leq \mathbb{E}_{(x,y) \sim \mathcal{D}}[\ell(f(x), y)] + B|\mu_i - \mu|_2 + B\sqrt{|\Sigma_i - \Sigma|_F}$$

This completes the proof. \square

Remark. Theorem 3.19 provides an insight into the performance of the empirical risk minimizer on a specific demographic group when the group's data distribution differs from the overall training distribution. The theorem shows that the excess risk of the empirical risk minimizer on group a_i can be bounded by three terms: (1) the excess risk of the empirical risk minimizer on the overall distribution, (2) the difference in means between the group-specific distribution and the overall distribution, and (3) the difference in covariance matrices between the group-specific distribution and the overall distribution. This result has important implications for understanding the sources of performance disparities across different demographic groups. It suggests that the accuracy of a model on a specific group depends not only on its performance on the overall population but also on how well the group's data distribution matches the overall training distribution. If the means and covariances of the group-specific distribution differ significantly from those of the overall distribution, the model may suffer from poor accuracy on that group [2]. The theorem assumes that the group-specific distribution follows a normal distribution, which is a common assumption in statistical modeling and analysis [42]. The use of the Euclidean distance between means and the Frobenius norm of the covariance matrix difference allows for a concise and interpretable bound on the excess risk. The insights from Theorem 3.19 can inform the development of fair and accurate models. They highlight the importance

of collecting representative data from each demographic group and considering the differences in data distributions when training and evaluating models [43]. Additionally, the theorem provides a way to quantify the impact of data distribution mismatch on the model’s performance, which can guide the development of targeted data collection and model improvement strategies [44].

Corollary 3.20 (Correlation between Expected Loss Bound and Feature Distance). *Let $\mathcal{D}_{a_i} \sim \mathcal{N}(\mu_i, \Sigma_i)$ be the data distribution for demographic group a_i , and let $\mathcal{D} \sim \mathcal{N}(\mu, \Sigma)$ be the overall data distribution. Let $f(\cdot)$ be a function that maps input x to a discriminative feature z in a metric space, and let ℓ be a loss function bounded by B , i.e., $|\ell(z, y)| \leq B$ for all z, y . Suppose we have a training set $(x_j, y_j)_{j=1}^n$ of size n drawn independently from \mathcal{D} . Let \bar{z} be the centroid of the features generated by f on the overall data distribution, and let \bar{z}_i be the centroid of the features generated by f on the demographic group a_i . Then, with probability at least $1 - \delta$, the expected loss of $f(\cdot)$ on \mathcal{D}_{a_i} is bounded as follows:*

$$\mathbb{E}_{(x,y) \sim \mathcal{D}_{a_i}}[\ell(f(x), y)] \leq \mathbb{E}_{(x,y) \sim \mathcal{D}}[\ell(f(x), y)] + B \cdot d(\bar{z}_i, \bar{z}) + B \sqrt{\mathbb{E}_{z \sim f(\mathcal{D}_{a_i})}[d^2(z, \bar{z}_i)] - \mathbb{E}_{z \sim f(\mathcal{D})}[d^2(z, \bar{z})]}$$

where $d(\cdot, \cdot)$ is a distance function in the metric space.

Proof. We start by applying Theorem 3.19 to the discriminative feature space:

$$\mathbb{E}_{(x,y) \sim \mathcal{D}_{a_i}}[\ell(f(x), y)] \leq \mathbb{E}_{(x,y) \sim \mathcal{D}}[\ell(f(x), y)] + B|\mu_{z_i} - \mu_z|_2 + B\sqrt{|\Sigma_{z_i} - \Sigma_z|_F}$$

where μ_{z_i} and Σ_{z_i} are the mean and covariance matrix of the features generated by f on \mathcal{D}_{a_i} , and μ_z and Σ_z are the mean and covariance matrix of the features generated by f on \mathcal{D} . By the definition of the centroid, we have $\bar{z}_i = \mu_{z_i}$ and $\bar{z} = \mu_z$. Therefore, $|\mu_{z_i} - \mu_z|_2 = d(\bar{z}_i, \bar{z})$. Now, let’s focus on the term $|\Sigma_{z_i} - \Sigma_z|_F$. By the properties of the Frobenius norm and the trace operator [45], we have:

$$\begin{aligned} & |\Sigma_{z_i} - \Sigma_z|_F \\ &= \sqrt{\text{tr}((\Sigma_{z_i} - \Sigma_z)^T(\Sigma_{z_i} - \Sigma_z))} \\ &= \sqrt{\text{tr}(\Sigma_{z_i}^2) - 2\text{tr}(\Sigma_{z_i}\Sigma_z) + \text{tr}(\Sigma_z^2)} \\ &= \sqrt{\mathbb{E}_{z \sim f(\mathcal{D}_{a_i})}[d^2(z, \bar{z}_i)] - 2\mathbb{E}_{z \sim f(\mathcal{D}_{a_i}), z' \sim f(\mathcal{D})}[d(z, z')] + \mathbb{E}_{z \sim f(\mathcal{D})}[d^2(z, \bar{z})]} \end{aligned}$$

Using the Cauchy-Schwarz inequality, we can bound the cross-term as follows:

$$\begin{aligned} \mathbb{E}_{z \sim f(\mathcal{D}_{a_i}), z' \sim f(\mathcal{D})}[d(z, z')] &\leq \sqrt{\mathbb{E}_{z \sim f(\mathcal{D}_{a_i})}[d^2(z, \bar{z}_i)] \cdot \mathbb{E}_{z \sim f(\mathcal{D})}[d^2(z, \bar{z})]} \\ &\leq \frac{1}{2} \left(\mathbb{E}_{z \sim f(\mathcal{D}_{a_i})}[d^2(z, \bar{z}_i)] + \mathbb{E}_{z \sim f(\mathcal{D})}[d^2(z, \bar{z})] \right) \end{aligned}$$

Substituting this bound into the expression for $|\Sigma_{z_i} - \Sigma_z|_F$, we get:

$$|\Sigma_{z_i} - \Sigma_z|_F \leq \sqrt{\mathbb{E}_{z \sim f(\mathcal{D}_{a_i})}[d^2(z, \bar{z}_i)] - \mathbb{E}_{z \sim f(\mathcal{D})}[d^2(z, \bar{z})]}$$

Combining the results for $|\mu_{z_i} - \mu_z|_2$ and $|\Sigma_{z_i} - \Sigma_z|_F$, we obtain the desired bound:

$$\begin{aligned} \mathbb{E}_{(x,y) \sim \mathcal{D}_{a_i}}[\ell(f(x), y)] &\leq \mathbb{E}_{(x,y) \sim \mathcal{D}}[\ell(f(x), y)] + B \cdot d(\bar{z}_i, \bar{z}) + \\ & B \sqrt{\mathbb{E}_{z \sim f(\mathcal{D}_{a_i})}[d^2(z, \bar{z}_i)] - \mathbb{E}_{z \sim f(\mathcal{D})}[d^2(z, \bar{z})]} \end{aligned}$$

This completes the proof. \square

Remark. Corollary 3.20 demonstrates that the expected loss bound for a demographic group a_i depends on three terms: (1) the expected loss on the overall data distribution, (2) the distance between the group-specific feature centroid

and the overall feature centroid, and (3) the difference in the average squared distances of the features from their respective centroids. This result highlights the importance of learning discriminative features that are well-clustered around their centroids and have similar distributions across different demographic groups [46]. By minimizing the distance between the group-specific centroids and the overall centroid, as well as reducing the discrepancy in the feature distributions, one can tighten the expected loss bound and achieve more equitable performance.

4 Experiments

Datasets. *FairVision* contains 30,000 2D scanning laser ophthalmoscopy (SLO) fundus images from 30,000 patients, and each patient has six demographic identity attributes available. This dataset features three common ophthalmic diseases: Diabetic Retinopathy (DR), Age-related Macular Degeneration (AMD), and Glaucoma, with 10,000 samples for each disease [11]. According to the official configuration, for each disease, 6,000 samples are used as the training set, 1,000 as the validation set, and 3,000 as the test set. We select the three demographic attributes, including race, gender, and ethnicity, with SLO fundus images as the focus of our study.

CheXpert is a large dataset of chest X-rays labeled for 14 common chest pathologies from associated radiologist reports. The dataset provides three demographic identity attributes: age, gender, and race [12]. Following the split setting in [47], [48], we select a total of 42,884 patients with 127,118 chest X-ray scans. Among these, 76,205 are used for the training set, 12,673 for the validation set, and 38,240 for the test set. In our experiments, we investigate the detection of pleural effusion across race and gender demographic attributes.

HAM10000, consisting of 10,015 dermatoscopic images, was collected over a span of 20 years from the Department of Dermatology at the Medical University of Vienna, Austria, and a dermatology practice in Queensland, Australia, providing a diverse and representative collection of pigmented skin lesions. Following [49], after filtering out images with missing sensitive attributes, we obtained a refined subset of 9,948 images, and grouped the original seven diagnostic labels into two categories: benign and malignant, to simplify the analysis and facilitate binary classification. For this study, we focus on gender and age as demographic attributes in the context of skin cancer detection.

FairFace is a newly curated dataset consisting of approximately 13,000 images from 3,000 new subjects, combined with a reannotated version of the IJB-C dataset [14], resulting in a total of 152,917 facial images from approximately 6,100 unique identities. The dataset is divided into three subsets: 100,186 images for training, 17,138 images for validation, and 35,593 images for testing. It is comprehensively annotated for protected attributes such as gender and skin color, as well as additional features including age group, eyeglasses, head pose, image source, and face size. In this study, we address glasses detection as a binary classification task, distinguishing images with and without eyeglasses, while focusing on the demographic attributes of age, skin color, and gender.

Implementation Details. We select two deep learning models with different frameworks as our baseline models:

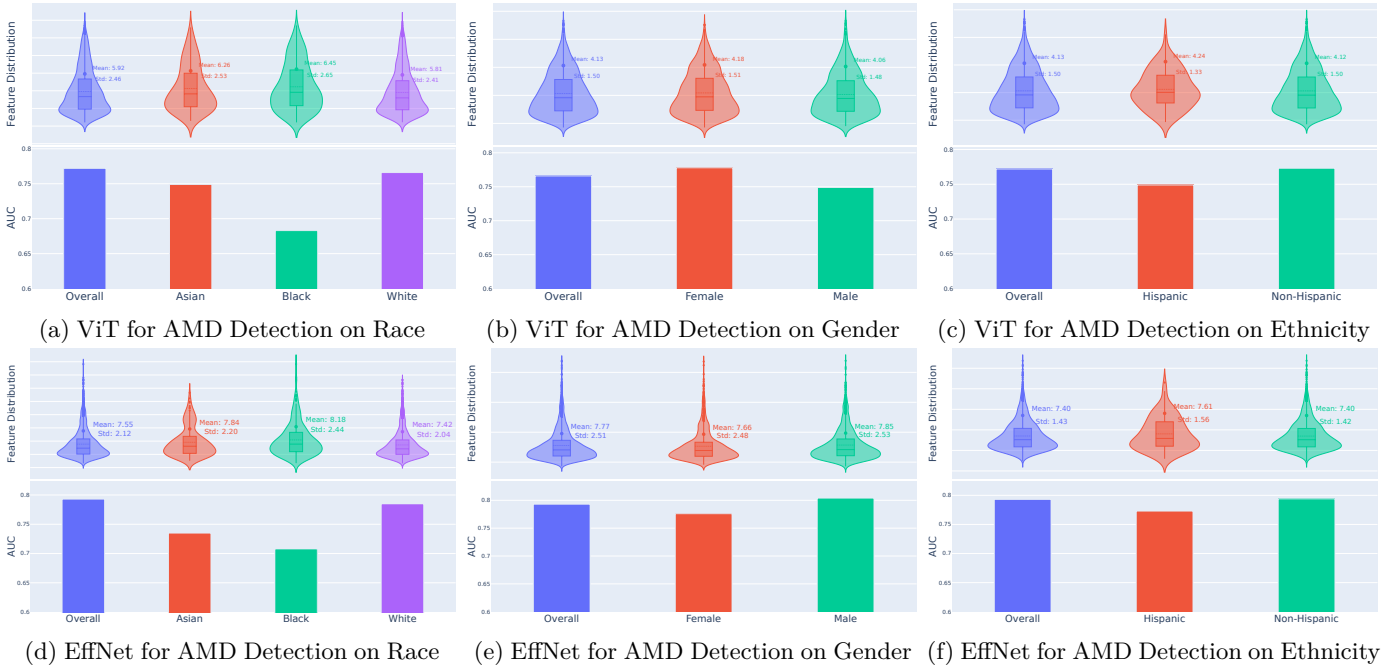


Fig. 1: Feature distribution and AUC comparison of ViT and EfficientNet for AMD detection across three demographic attributes, including Race, Gender, and Ethnicity, on **FairVision** dataset

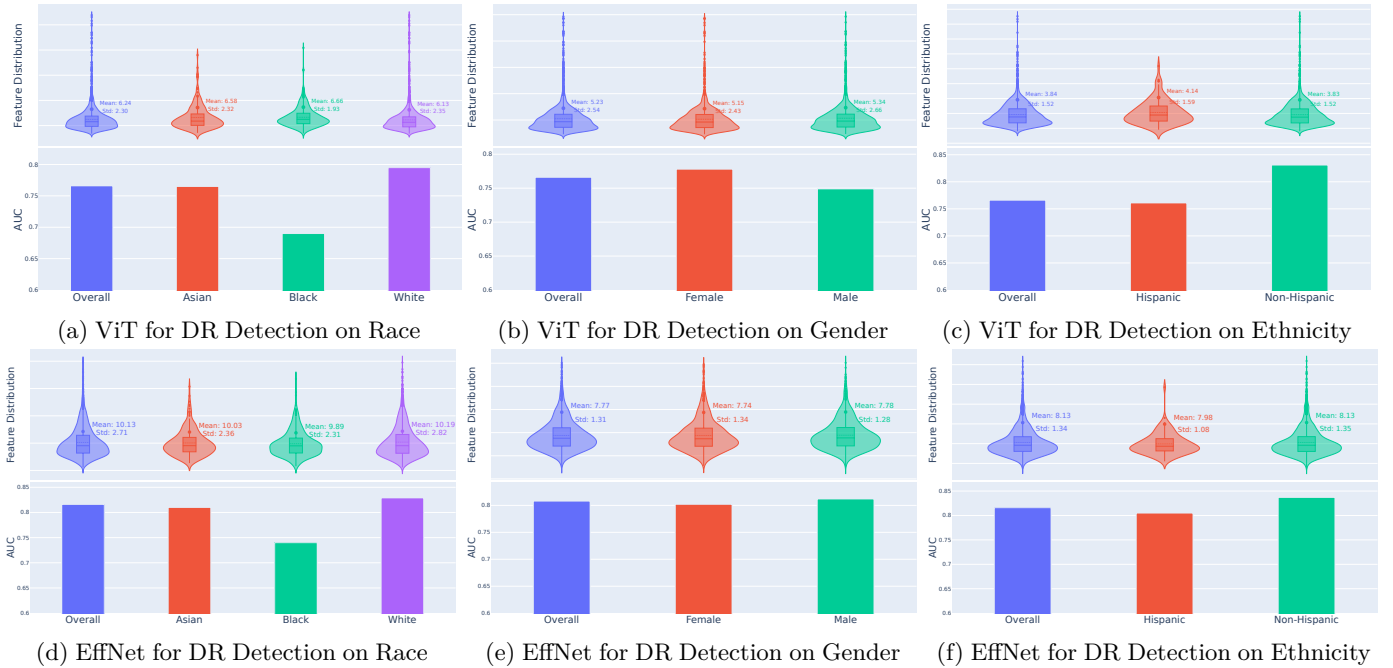


Fig. 2: Feature distribution and AUC comparison of ViT and EfficientNet for DR detection across three demographic attributes, including Race, Gender, and Ethnicity, on **FairVision** dataset

the CNN-based EfficientNet [50] and the Transformer-based ViT [51]. All experiments are conducted on an A100 GPU with 80GB of memory. We initialize both EfficientNet and ViT using pre-trained weights provided by TorchVision. During the fine-tuning phase, EfficientNet is trained for 10 epochs with a learning rate of $1e-4$ and a batch size of 10. Similarly, ViT is trained for 10 epochs with a learning rate of $1e-4$ and a batch size of 50.

Results. We first trained ViT and EfficientNet models on

the training sets of the FairVision dataset for detecting DR, AMD, and Glaucoma. After training, the models were applied to the corresponding test sets, where we obtained the encoded features and predicted labels. Using these outputs, we calculated the Euclidean distance of the features to the mean, representing the empirical feature distribution, and evaluated the Area Under the Curve (AUC) accuracy for both the overall and individual demographic groups. The feature distributions and AUC results for DR, AMD, and

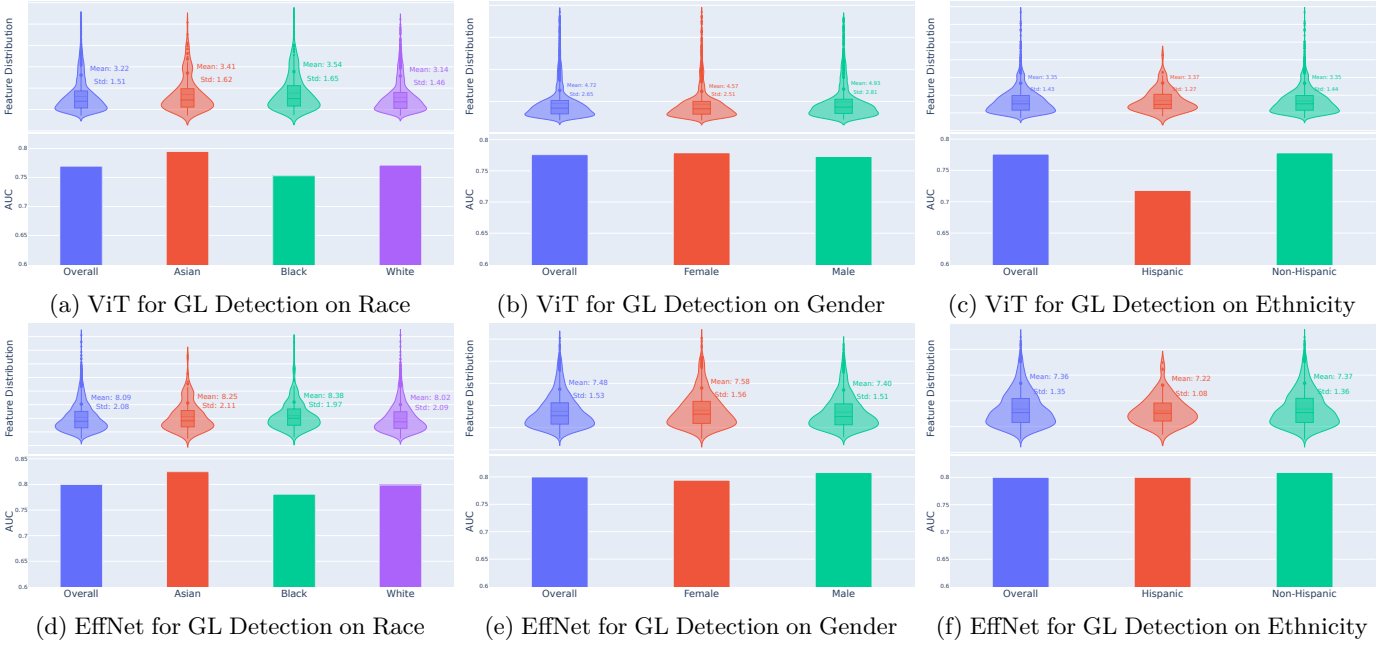


Fig. 3: Feature distribution and AUC comparison of ViT and EfficientNet for Glaucoma (GL) detection across three demographic attributes, including Race, Gender, and Ethnicity, on **FairVision** dataset.

Glaucoma detection are illustrated in Fig. 1, Fig. 2, and Fig. 3. From the figures, it is evident that both models achieved reasonable detection performance across all three diseases, with EfficientNet consistently outperforming ViT in terms of accuracy. Additionally, we observed significant disparities in AUC values across different demographic groups, underscoring the importance of studying fairness in AI systems. These disparities are particularly pronounced in the results stratified by race, where the Black group exhibits significantly lower detection accuracy compared to the Asian and White groups across all three diseases.

Furthermore, we extended our experiments to the CheXpert, HAM10000, and FairFace datasets to evaluate model performance on additional medical imaging and facial recognition tasks. Considering the superior performance of EfficientNet on the FairVision dataset compared to ViT, we primarily focused on EfficientNet’s performance across demographic groups in these datasets. The results for CheXpert, HAM10000, and FairFace are presented in Fig. 4, Fig. 5, and Fig. 6, respectively. From the results, it is apparent that detection performance also varies significantly across different demographic groups in these datasets. For instance, in the CheXpert dataset, disparities in AUC are observed when analyzing pleural effusion detection performance across race and gender attributes. Similarly, for HAM10000, detection of skin lesions exhibits performance variations across age and gender groups. In the FairFace dataset, the performance of eyeglass detection also shows notable differences among subgroups defined by age, skin color, and gender.

Discussion. Our experimental results across multiple datasets demonstrate the relationship between data distributions and fairness guarantees as predicted by Theorem 3.19 and Corollary 3.20. Let’s analyze the results for each dataset:

FairVision Dataset For AMD detection (Fig. 1), both ViT and EfficientNet show significant performance variations across demographic groups. With ViT, the overall feature distribution has a mean of 5.92 and standard deviation of 2.46. The Asian group (mean: 6.26, std: 2.53) and Black group (mean: 6.45, std: 2.65) show larger deviations from the overall distribution compared to the White group (mean: 5.81, std: 2.41). According to Theorem 3.19, this translates to potentially higher expected loss for these groups:

For the Asian group:

$$E_{(x,y) \sim D_{Asian}}[\ell(f(x), y)] \leq E_{(x,y) \sim D}[\ell(f(x), y)] + 0.34B + 0.07B$$

For the Black group:

$$E_{(x,y) \sim D_{Black}}[\ell(f(x), y)] \leq E_{(x,y) \sim D}[\ell(f(x), y)] + 0.53B + 0.19B$$

Similar patterns emerge for DR detection (Fig. 2), where the Black group shows the largest deviation (mean: 6.66, std: 1.93) from the overall distribution (mean: 6.24, std: 2.30), corresponding to lower AUC values. For Glaucoma detection (Fig. 3), the feature distribution differences are particularly pronounced between racial categories, with the Black group consistently showing the largest deviation and correspondingly lower performance.

CheXpert Dataset The results for pleural effusion detection (Fig. 4) demonstrate how distributional differences affect fairness across both race and gender. The feature distributions show notable variations, with the Black group exhibiting the largest deviation (mean: 11.50, std: 7.43) from the overall distribution (mean: 10.85, std: 6.21). This aligns with Corollary 3.20, which predicts larger expected loss bounds when feature centroids are more distant from the overall centroid.

HAM10000 Dataset For skin cancer detection (Fig. 5), the age-based disparities are particularly notable. The feature distribution for patients aged ≥ 60 (mean: 12.43, std: 4.16)

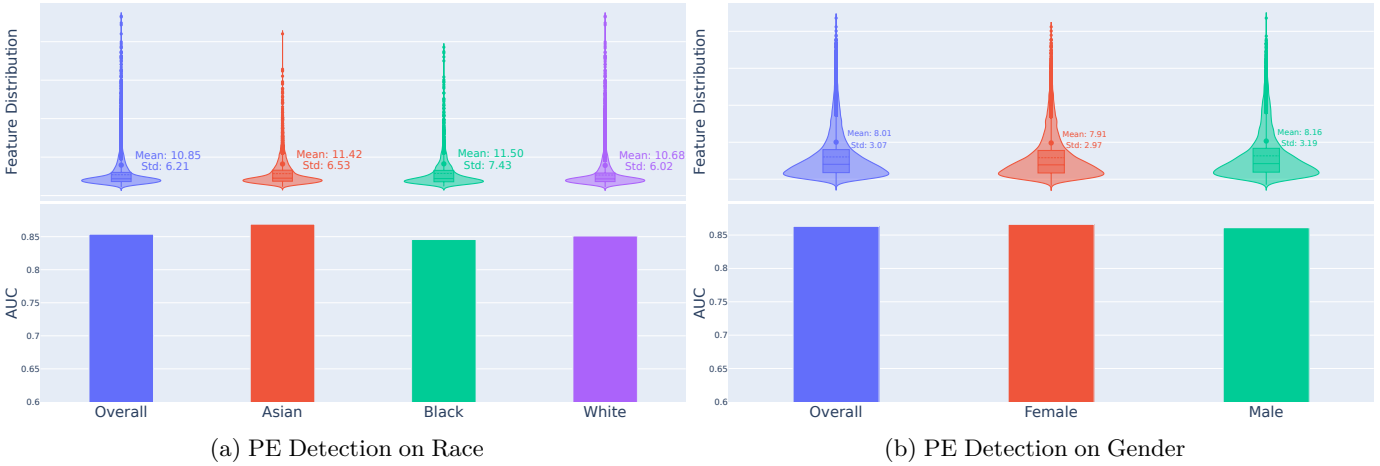


Fig. 4: Feature distribution and AUC comparison of EfficientNet for Pleural Effusion (PE) detection across two demographic attributes, including Race and Gender, on **Chexpert** dataset.

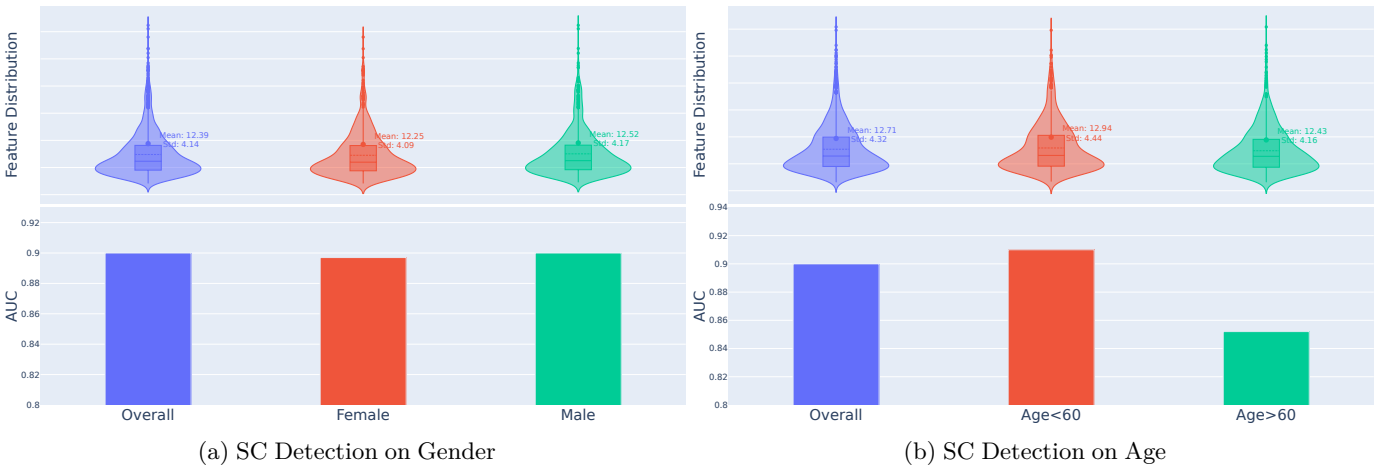


Fig. 5: Feature distribution and AUC comparison of EfficientNet for Skin Cancer (SC) detection across two demographic attributes, including Gender and Age, on **HAM10000** dataset.

differs significantly from the overall distribution (mean: 12.71, std: 4.32), leading to performance disparities that align with our theoretical predictions about the relationship between distribution differences and fairness guarantees.

FairFace Dataset The glasses detection results (Fig. 6) show how multiple demographic attributes interact with fairness guarantees. The feature distributions vary across age groups, skin color, and gender, with the age>65 group showing the largest deviation (mean: 10.29, std: 2.74) from the overall distribution (mean: 10.21, std: 2.45). This multi-attribute variation demonstrates the complexity of achieving fairness when dealing with intersectional demographic characteristics.

These empirical results consistently support our theoretical framework, showing that groups with feature distributions deviating significantly from the overall distribution tend to experience lower performance. The relationship between distribution differences and fairness guarantees is particularly evident in:

- 1) The consistent correlation between feature distribution deviation and AUC performance across all datasets

- 2) The more pronounced fairness issues in racial categories, where distribution differences tend to be larger
- 3) The compounding effects when multiple demographic attributes deviate from the overall distribution

The results also validate the practical utility of our theoretical bounds in predicting and understanding fairness disparities.

5 Conclusion

This work presents a theoretical analysis of the impact of data distributions on the fairness guarantees of deep learning models. Our analysis reveals that fairness is fundamentally constrained by the distributional differences between demographic groups, as demonstrated through our derived bounds on fairness errors, convergence rates, and group-specific risks. These theoretical insights are validated through extensive experiments on multiple datasets, where groups with feature distributions deviating significantly from the overall distribution consistently show lower performance, particularly across racial categories.

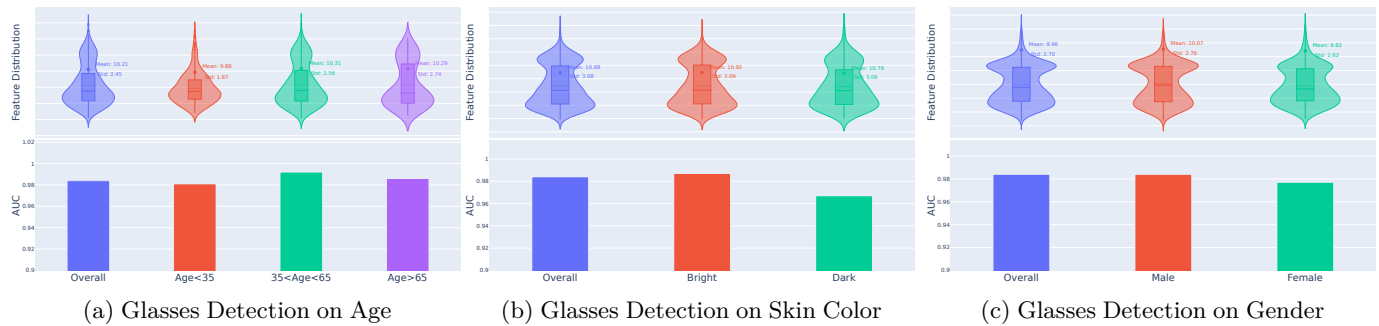


Fig. 6: Feature distribution and AUC comparison of EfficientNet for Glasses detection across three demographic attributes, including Age, Skin Color, and Gender, on **FairFace** dataset.

References

[1] A. Rajkomar, M. Hardt, M. D. Howell, G. Corrado, and M. H. Chin, “Ensuring fairness in machine learning to advance health equity,” *Annals of internal medicine*, vol. 169, no. 12, pp. 866–872, 2018.

[2] I. Chen, F. D. Johansson, and D. Sontag, “Why is my classifier discriminatory?” *Advances in neural information processing systems*, vol. 31, 2018.

[3] L. Oakden-Rayner, J. Dunnmon, G. Carneiro, and C. Ré, “Hidden stratification causes clinically meaningful failures in machine learning for medical imaging,” in *Proceedings of the ACM conference on health, inference, and learning*, 2020, pp. 151–159.

[4] D. Zietlow, M. Lohaus, G. Balakrishnan, M. Kleindessner, F. Locatello, B. Schölkopf, and C. Russell, “Leveling down in computer vision: Pareto inefficiencies in fair deep classifiers,” in *Proceedings of the IEEE/CVF Conference on Computer Vision and Pattern Recognition*, 2022, pp. 10 410–10 421.

[5] C. Dwork, M. Hardt, T. Pitassi, O. Reingold, and R. Zemel, “Fairness through awareness,” in *Proceedings of the 3rd innovations in theoretical computer science conference*, 2012, pp. 214–226.

[6] A. Agarwal, A. Beygelzimer, M. Dudík, J. Langford, and H. Wallach, “A reductions approach to fair classification,” in *International conference on machine learning*. PMLR, 2018, pp. 60–69.

[7] M. B. Zafar, I. Valera, M. Gomez Rodriguez, and K. P. Gummadi, “Fairness beyond disparate treatment & disparate impact: Learning classification without disparate mistreatment,” in *Proceedings of the 26th international conference on world wide web*, 2017, pp. 1171–1180.

[8] A. Chouldechova, “Fair prediction with disparate impact: A study of bias in recidivism prediction instruments,” *Big data*, vol. 5, no. 2, pp. 153–163, 2017.

[9] S. Corbett-Davies, E. Pierson, A. Feller, S. Goel, and A. Huq, “Algorithmic decision making and the cost of fairness,” in *Proceedings of the 23rd acm sigkdd international conference on knowledge discovery and data mining*, 2017, pp. 797–806.

[10] S. Hajian, J. Domingo-Ferrer, A. Monreale, D. Pedreschi, and F. Giannotti, “Discrimination-and privacy-aware patterns,” *Data Mining and Knowledge Discovery*, vol. 29, no. 6, pp. 1733–1782, 2015.

[11] Y. Luo, Y. Tian, M. Shi, T. Elze, and M. Wang, “Fairvision: Equitable deep learning for eye disease screening via fair identity scaling,” *arXiv preprint arXiv:2310.02492*, 2023.

[12] J. Irvin, P. Rajpurkar, M. Ko, Y. Yu, S. Ciurea-Ilcus, C. Chute, H. Marklund, B. Haghgoo, R. Ball, K. Shpanskaya *et al.*, “Chexpert: A large chest radiograph dataset with uncertainty labels and expert comparison,” in *Proceedings of the AAAI conference on artificial intelligence*, vol. 33, no. 01, 2019, pp. 590–597.

[13] P. Tschandl, C. Rosendahl, and H. Kittler, “The ham10000 dataset, a large collection of multi-source dermatoscopic images of common pigmented skin lesions,” *Scientific data*, vol. 5, no. 1, pp. 1–9, 2018.

[14] B. Maze, J. Adams, J. A. Duncan, N. Kalka, T. Miller, C. Otto, A. K. Jain, W. T. Niggel, J. Anderson, J. Cheney *et al.*, “Iarpa janus benchmark-c: Face dataset and protocol,” in *2018 international conference on biometrics (ICB)*. IEEE, 2018, pp. 158–165.

[15] Z. Wang, K. Qinami, I. C. Karakozis, K. Genova, P. Nair, K. Hata, and O. Russakovsky, “Towards fairness in visual recognition: Effective strategies for bias mitigation,” in *Proceedings of the IEEE/CVF conference on computer vision and pattern recognition*, 2020, pp. 8919–8928.

[16] F. Kamiran and T. Calders, “Data preprocessing techniques for classification without discrimination,” *Knowledge and information systems*, vol. 33, no. 1, pp. 1–33, 2012.

[17] M. Ngxande, J.-R. Tapamo, and M. Burke, “Bias remediation in driver drowsiness detection systems using generative adversarial networks,” *IEEE Access*, vol. 8, pp. 55 592–55 601, 2020.

[18] T. Xu, J. White, S. Kalkan, and H. Gunes, “Investigating bias and fairness in facial expression recognition,” in *Computer Vision–ECCV 2020 Workshops: Glasgow, UK, August 23–28, 2020, Proceedings, Part VI 16*. Springer, 2020, pp. 506–523.

[19] M. Hardt, E. Price, and N. Srebro, “Equality of opportunity in supervised learning,” *Advances in neural information processing systems*, vol. 29, 2016.

[20] G. Pleiss, M. Raghavan, F. Wu, J. Kleinberg, and K. Q. Weinberger, “On fairness and calibration,” *Advances in neural information processing systems*, vol. 30, 2017.

[21] Z. Lipton, J. McAuley, and A. Chouldechova, “Does mitigating ml’s impact disparity require treatment disparity?” *Advances in neural information processing systems*, vol. 31, 2018.

[22] T. Jang, H. Gao, P. Shi, and X. Wang, “Achieving fairness through separability: A unified framework for fair representation learning,” in *International Conference on Artificial Intelligence and Statistics*. PMLR, 2024, pp. 28–36.

[23] A. Asuncion and D. Newman, “Uci machine learning repository,” 2007.

[24] S. Ruggles, R. McCaa, M. Sobek, and L. Cleveland, “The ipums collaboration: integrating and disseminating the world’s population microdata,” *Journal of demographic economics*, vol. 81, no. 2, pp. 203–216, 2015.

[25] J. Dressel and H. Farid, “The accuracy, fairness, and limits of predicting recidivism,” *Science advances*, vol. 4, no. 1, p. eaao5580, 2018.

[26] A. C. McGinley, “Ricci v. destefano: A masculinities theory analysis,” *Harv. JL & Gender*, vol. 33, p. 581, 2010.

[27] W. Miao, “Did the results of promotion exams have a disparate impact on minorities? using statistical evidence in ricci v. destefano,” *Journal of Statistics Education*, vol. 18, no. 3, 2010.

[28] J. Kuzilek, M. Hlosta, and Z. Zdrahal, “Open university learning analytics dataset,” *Scientific data*, vol. 4, no. 1, pp. 1–8, 2017.

[29] A. E. Johnson, T. J. Pollard, N. R. Greenbaum, M. P. Lungren, C.-y. Deng, Y. Peng, Z. Lu, R. G. Mark, S. J. Berkowitz, and S. Horng, “Mimic-cxr-jpg, a large publicly available database of labeled chest radiographs,” *arXiv preprint arXiv:1901.07042*, 2019.

[30] O. Kovalyk, J. Morales-Sánchez, R. Verdú-Monedero, I. Sellés-Navarro, A. Palazón-Cabanes, and J.-L. Sancho-Gómez, “Papila: Dataset with fundus images and clinical data of both eyes of the same patient for glaucoma assessment,” *Scientific Data*, vol. 9, no. 1, p. 291, 2022.

[31] M. Groh, C. Harris, L. Soenksen, F. Lau, R. Han, A. Kim, A. Koochek, and O. Badri, “Evaluating deep neural networks

- trained on clinical images in dermatology with the fitzpatrick 17k dataset,” in *Proceedings of the IEEE/CVF Conference on Computer Vision and Pattern Recognition*, 2021, pp. 1820–1828.
- [32] J. M. Zambrano Chaves, A. S. Chaudhari, A. L. Wentland, A. D. Desai, I. Banerjee, R. D. Boutin, D. J. Maron, F. Rodriguez, A. T. Sandhu, R. B. Jeffrey *et al.*, “Opportunistic assessment of ischemic heart disease risk using abdominopelvic computed tomography and medical record data: a multimodal explainable artificial intelligence approach,” *medRxiv*, pp. 2021–01, 2021.
- [33] P. Afshar, S. Heidarian, N. Enshaei, F. Naderkhani, M. J. Rafiee, A. Oikonomou, F. B. Fard, K. Samimi, K. N. Plataniotis, and A. Mohammadi, “Covid-ct-md, covid-19 computed tomography scan dataset applicable in machine learning and deep learning,” *Scientific Data*, vol. 8, no. 1, p. 121, 2021.
- [34] S. Farsiu, S. J. Chiu, R. V. O’Connell, F. A. Folgar, E. Yuan, J. A. Izatt, C. A. Toth, A.-R. E. D. S. . A. S. D. O. C. T. S. Group *et al.*, “Quantitative classification of eyes with and without intermediate age-related macular degeneration using optical coherence tomography,” *Ophthalmology*, vol. 121, no. 1, pp. 162–172, 2014.
- [35] B. T. Wyman, D. J. Harvey, K. Crawford, M. A. Bernstein, O. Carmichael, P. E. Cole, P. K. Crane, C. DeCarli, N. C. Fox, J. L. Gunter *et al.*, “Standardization of analysis sets for reporting results from adni mri data,” *Alzheimer’s & Dementia*, vol. 9, no. 3, pp. 332–337, 2013.
- [36] M. Donini, L. Oneto, S. Ben-David, J. S. Shawe-Taylor, and M. Pontil, “Empirical risk minimization under fairness constraints,” *Advances in neural information processing systems*, vol. 31, 2018.
- [37] S. Shalev-Shwartz and S. Ben-David, *Understanding machine learning: From theory to algorithms*. Cambridge university press, 2014.
- [38] A. W. Van Der Vaart and J. A. Wellner, *Weak convergence and empirical processes: with applications to statistics*. Springer New York, 1997.
- [39] V. N. Vapnik, “An overview of statistical learning theory,” *IEEE transactions on neural networks*, vol. 10, no. 5, pp. 988–999, 1999.
- [40] L. Bottou and O. Bousquet, “The tradeoffs of large scale learning,” *Advances in neural information processing systems*, vol. 20, 2007.
- [41] C. R. Givens and R. M. Shortt, “A class of wasserstein metrics for probability distributions,” *Michigan Mathematical Journal*, vol. 31, no. 2, pp. 231–240, 1984.
- [42] K. P. Murphy, *Machine learning: a probabilistic perspective*. MIT press, 2012.
- [43] J. Buolamwini and T. Gebru, “Gender shades: Intersectional accuracy disparities in commercial gender classification,” in *Conference on fairness, accountability and transparency*. PMLR, 2018, pp. 77–91.
- [44] M. Kearns, S. Neel, A. Roth, and Z. S. Wu, “Preventing fairness gerrymandering: Auditing and learning for subgroup fairness,” in *International conference on machine learning*. PMLR, 2018, pp. 2564–2572.
- [45] F. Zhang, *Matrix theory: basic results and techniques*. Springer Science & Business Media, 2011.
- [46] R. Zemel, Y. Wu, K. Swersky, T. Pitassi, and C. Dwork, “Learning fair representations,” in *International conference on machine learning*. PMLR, 2013, pp. 325–333.
- [47] J. W. Gichoya, I. Banerjee, A. R. Bhimireddy, J. L. Burns, L. A. Celi, L.-C. Chen, R. Correa, N. Dullerud, M. Ghassemi, S.-C. Huang *et al.*, “Ai recognition of patient race in medical imaging: a modelling study,” *The Lancet Digital Health*, vol. 4, no. 6, pp. e406–e414, 2022.
- [48] B. Glocker, C. Jones, M. Bernhardt, and S. Winzeck, “Algorithmic encoding of protected characteristics in chest x-ray disease detection models,” *EBioMedicine*, vol. 89, 2023.
- [49] Y. Zong, Y. Yang, and T. Hospedales, “Medfair: Benchmarking fairness for medical imaging,” *arXiv preprint arXiv:2210.01725*, 2022.
- [50] M. Tan and Q. Le, “Efficientnet: Rethinking model scaling for convolutional neural networks,” in *International conference on machine learning*. PMLR, 2019, pp. 6105–6114.
- [51] A. Dosovitskiy, L. Beyer, A. Kolesnikov, D. Weissenborn, X. Zhai, T. Unterthiner, M. Dehghani, M. Minderer, G. Heigold, S. Gelly *et al.*, “An image is worth 16x16 words: Transformers for
- image recognition at scale,” *arXiv preprint arXiv:2010.11929*, 2020.